A major purpose of the Technical Information Center is to provide the broadest dissemination possible of information contained in DOE's Research and Development Reports to business, industry, the academic community, and federal, state and local governments.

Although a small portion of this report is not reproducible, it is being made available to expedite the availability of information on the research discussed herein.

CONF-860667--7

Los Alamos National Laboratory is operated by the University of California for the United States Department of Energy under contract W-7405-ENG-36

TITLE: Seismic Monitoring of Hydraulic Fracturing: Techniques for Determining Fluid Flow Paths and State of Stress Away from a Wellbore

LA-UR -86-785

DE86 007365

AUTHOR(S): Michael Fehler
Leigh House
Hideshi Kaieda

SUBMITTED TO

27th U.S. Symposium on Rock Mechanics
(to be held at the University of Alabama
on 23-25 June, 1986)

MASTER

Los Alamos Los Alamos National Laboratory
Los Alamos, New Mexico 87545

Seismic Monitoring of Hydraulic Fracturing: Techniques for Determining Fluid Flow Paths and State of Stress Away From a Wellbore

Michael Fehler, Leigh House and Hideshi Kaieda[1]

Earth and Space Sciences Division, Los Alamos National Laboratory Los Alamos, New Mexico 87545
[1] Visiting Scientist, Central Research Institute of the Electric Power Industry, Chiba, Japan

ABSTRACT

Hydraulic fracturing has gained in popularity in recent years as a way to determine the orientations and magnitudes of tectonic stresses. By supplementing conventional hydraulic fracturing measurements with detection and mapping of the microearthquakes induced by fracturing, we can supplement and independently confirm information obtained from conventional analysis. Important information obtained from seismic monitoring includes: the state of stress of the rock, orientation and spacing of the major joint sets, and measurements of rock elastic parameters at locations distant from the wellbore. While conventional well logging operations can provide information about several of these parameters, the zone of interrogation is usually limited to the immediate proximity of the borehole.

The seismic waveforms of the microearthquakes contain a wealth of information about the rock in regions that are otherwise inaccessible for study. By reliably locating the hypocenters of many microearthquakes, we have inferred the joint patterns in the rock. We observed that microearthquake locations do not define a simple, thin, planar distribution, that the fault plane solutions are consistent with shear slippage, and that spectral analysis indicates that the source dimensions and slip along the faults are small. Hence we believe that the microearthquakes result from slip along preexisting joints, and not from tensile extension at the tip of the fracture. Orientations of the principal stresses can be estimated by using fault plane solutions of the larger microearthquakes. By using a joint earthquake location scheme, and/or calibrations with downhole detonators, rock velocities and heterogeneities thereof can be investigated in rock volumes that are far enough from the borehole to be representative of intact rock properties.

INTRODUCTION

In studies of earth stress by hydraulic fracturing, a small amount of fluid is injected at the depth selected for study and the pressure record vs. time is recorded. The magnitude of the least principal stress is determined directly from the pressure record (Haimson and Rummel, 1982; Stock, et al, 1985). The magnitude of the maximum principal stress can be determined from the pressure record and a knowledge of the fracture properties of the rock. The directions of the principal stresses are then determined by using an impression packer or televiewer to measure the orientation of the tensile fracture induced by the fracturing, which is assumed to be orthogonal to the least principal stress direction.

Cornet and Valette(1985) have pointed out some of the difficulties with hydraulic fracturing measurements of stress in rock containing pre-existing joints and proposed a technique to use the existence of the joints to advantage to actually measure the complete stress tensor. The technique requires that joints of various orientations be identified and subsequently opened by hydraulic injections.

We have found that hydraulic fracturing of crystalline rocks is accompanied by a substantial number of microearthquakes that can be recorded and subsequently studied to yield additional information about the state of the rock away from the borehole. By determining the locations of the microearthquakes we determine preferential directions of fluid flow paths, which appear to follow pre-existing joints in the rock. Statistical analysis of the relative three dimensional locations of the microearthquakes determines the dips and azimuths of these major joints. Fault plane solutions determined for the larger events provide information about the state of stress in the rock. If a sufficient number of fault plane solutions can be determined, they can be modeled to determine the ratios of the magnitudes of the principal stresses. In this way, the state of stress of the rock can be determined at locations well removed from the borehole, where stress results are not influenced by the presence of the borehole.

Source parameters of individual microearthquakes such as stress drop, seismic moment,

displacement, and the area of the joint mobilized in an individual microquake can be determined from the spectra of the waveforms. We find that the amount of displacement along the joint during a microearthquake is small, which means that there is little increase in permeability due to the microearthquake.

Travel times of the seismic waves from the microearthquake source to the recording stations can be inverted to place limits on the heterogeneity of the rock in the region in and near where the microearthquakes are occurring. By studying the particle motion of the S waves recorded by three component geophones, it is also possible to determine preferential orientations of microcracks in the rock (e.g. rock anisotropy) (Roberts and Crampin, 1986).

In this paper, we discuss the results of analysis of seismic data collected during a massive hydraulic fracturing experiment conducted in the Jemez Mountains in New Mexico by the Los Alamos Hot Dry Rock Geothermal Energy project. A total of 21,60[illegible] m³ of water were injected during this experiment. Nearly 2 million microearthquakes were detected, most of which were far too small to be studied. While this large experiment was chosen for detailed study because of its large size and significance to the Hot Dry Rock project, we have also successfully analyzed much smaller fluid injections. For example, fault plane solutions from an experiment in which only 900 m³ of water were injected have been published by Cash et al (1988).

Seismic results of other hydraulic fracture experiments include those by Albright and Hanold (1976), Albright and Pearson (1982), Pearson (1981, 1982), Rutledge, et al (1987), Pine and Batchelor (1984), and House, et al (1985).

THE MASSIVE HYDRAULIC FRACTURING EXPERIMENT

In December, 1983, a hydraulic fracturing experiment (termed experiment 2032) was carried out at the Hot Dry Rock Geothermal Energy Development test site at Fenton Hill, New Mexico. A total of 21,600 m³ of water were injected into a 270 m long open-hole section of the lower of two inclined wells, EE-2, at a depth of 3900 m. Injection was carried out over a time interval of 60 hours at an average wellhead pressure of 48 MPa and injection rate of .1 m³/s.

Downhole monitoring of the induced seismicity was conducted with three triaxial geophone tools, all located within a few hundred meters of the seismic activity. In addition, two vertical component geophone tools were located at distances of several kilometers from the injection point, and a network of nine surface seismic stations was deployed at distances ranging up to 10 kilometers from the injection point. Figures 1 and 2 are map views showing the locations of the downhole and surface sensors, respectively, and the location of wellbore EE-2. All seismic data were recorded on analog magnetic tape, and digital data from the

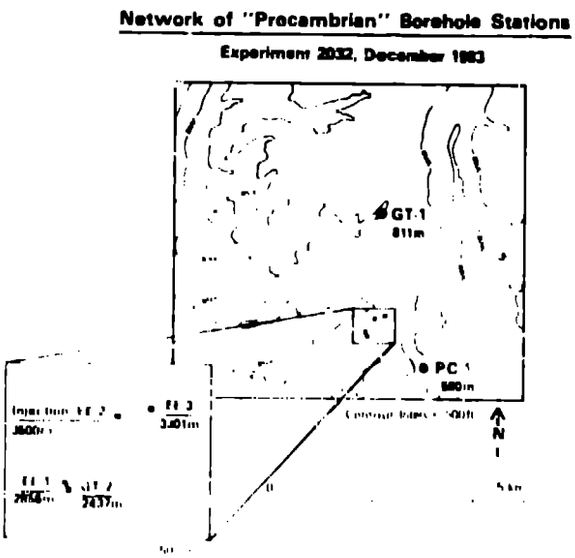

Figure 1. Plan view of the Precambrian seismic network used to monitor the hydraulic fracturing experiment. Three component sensors were located in boreholes EE-1, EE-3 and GT-2. Vertical sensors were located in boreholes PC-1 and GT-1. Depths of sensors are given as distances along the wellbore.

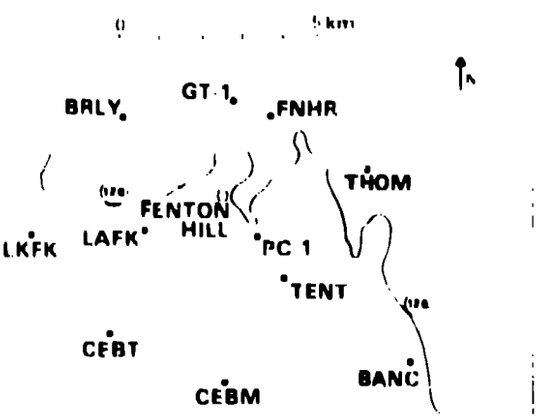

Figure 2. Plan view of the Fenton Hill surface seismic network. All stations employ vertical component 1 Hz velocity sensors.

downhole geophones were obtained from about 1800 seismic events during the 84 hours that seismic monitoring was carried out.

The water was injected into Precambrian granites and granodiorites. Seismic ray paths to the close-in triaxial borehole sensors were entirely within the granites, whose seismic velocities appear to be relatively homogeneous and isotropic. In contrast, raypaths to the surface seismic sensors, and to a lessor extent, the outlying single component sensors, were distorted by lower velocity sediments that extend from the surface to a depth of approximately 700 m.

MICROEARTHQUAKE LOCATIONS

Data from all five downhole instruments were used to obtain locations of seismic events by inversion of arrival times of the compressional (P) and shear (S) waves. Arrival times were determined from digital seismograms with a precision of 1 ms. Seismic velocities and average station corrections were obtained from detonator calibration shots placed in the boreholes and a suite of well recorded microearthquakes; the average P velocity is 5.92 km/s and the S wave velocity is 3.50 km/s. Station corrections compensate for the slight observed variations from the constant velocity model. Individual station corrections were found to be only a very small fraction of the travel times to the stations (less than a few percent), which supports our assertion that the rock velocity is nearly homogeneous. The only exception was for station PC-1, which was located some 200 m above the sediment-granite interface, and hence the travel path to this station is not entirely through homogeneous rock.

Of the 1800 events that were digitized during the experiment, 844 were located with computed locational errors of less than 50 m. A plan view, or epicenter map, of these events is shown in Figure 3. We estimate that the precision of the locations (e.g. difference in relative locations) is 10-20 m and the uncertainty in absolute locations is probably no greater than 50-100 m. The great precision of the locations makes it possible to study the relative locations to determine if lineaments such as lengthy joints can be detected.

FAULT PLANE SOLUTIONS AND REGIONAL STRESSES

Signals recorded at the nine surface stations and at the two outlying downhole stations were used to study fault plane solutions. Since seismic waves arriving at the surface stations must pass through approximately 700 m of highly attenuating sediments, only the larger (magnitudes ranging from -2 to 0) events accompanying the injection could be studied using this network. Of the more than 1000 events recorded by the surface network, 69 of the most suitable were chosen for study.

In order to reliably determine take off angles of seismic waves to the various stations, the events had to be located. Since data from the

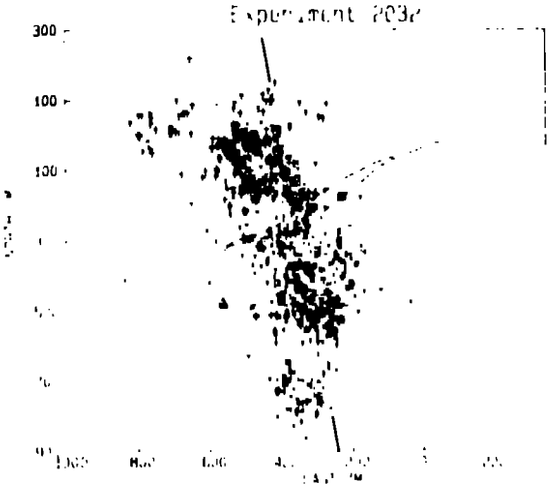

Figure 3. Map view of locations of seismic events accompanying the hydraulic fracturing experiment. The location of the three component seismic sensor in EE-1 is indicated by the solid triangle, that in EE-3 by a solid square. In map view, the location of the instrument in GT-2 is nearly identical to that in EE-1. The strike of the seismic cloud, 150°, is indicated by the lines at top and bottom of the figure. Precision of event locations is about 10-20 m, about the size of the event symbols.

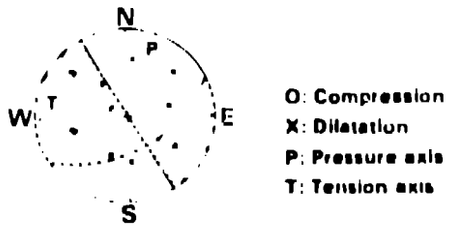

Fault Plane Solution of Group I
Lower hemisphere projection

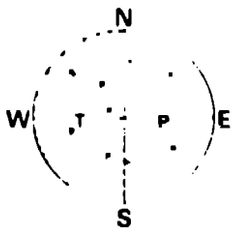

Fault Plane Solution of Group II
Lower hemisphere projection

Figure 4. Fault plane solutions that were found most often in the hydraulic fracturing data set. Points in focal spheres indicate the station locations and the measured polarity of first motion. Lower hemisphere projections are shown.

surface network were not recorded digitally at the time of the experiment, the data from larger events recorded by both the surface and downhole networks were digitized after the experiment. In this way, events could be located using only the travel times to the downhole stations, which have greater precision than those to the surface network stations.

Directions of first motions of the 69 events show both compressions and dilitations and, although many different focal mechanisms were determined, all are consistent with shear slip. Of the 31 events for which reliable fault plane solutions were determined, 19 have one of two fault plane solutions. These two most common solutions are plotted in Figure 4. Note that the difference between the two fault plane solutions results entirely from a difference in first motion at a single station. Since the change in first motion is clear on the seismograms, and since mislocation of the events cannot move the position of the station on the focal sphere enough to account for the observed differences, the difference in fault plane solutions is real. The events with the two focal mechanisms shown in Figure 4 occur throughout the region where seismic events were located. Moreover, the events that exhibit fault plane solutions different from those shown are also located throughout the seismic zone.

Of the seven types of fault plane solutions found for the seismic events studied, all have one feature in common; a nearly vertical N-S or NW-SE striking nodal plane. This nearly vertical nodal plane is sub-parallel to the trend of the seismic zone, which has an azimuth of approximately 350° and a dip of 75° (see line drawn in Figure 4). In addition, the T axes for the seven solutions trend roughly east-west and are in reasonable accord with the regional stress observations of Aldrich and Laughlin (1984).

The two solutions shown in Figure 4 are almost identical to composite fault plane solutions obtained by Cash et al(1983; note that they plot upper hemisphere projections) although they found the two solutions from events separated by 1 km of depth. They proposed a spatial difference in regional stresses associated with the nearby Valles Caldera as an explanation for the differences in the two fault plane solutions. Since the events studied here are in very close proximity, it is unlikely that they can be due to spatial differences in regional stresses. Rather, they most likely result from the same stress field. Recent work by Gephart and Forsyth (1984), Michael (1984), and others have shown that suites of fault plane solutions for earthquakes occurring in one region, and hence considered as being due to a single uniform stress field, can be inverted to determine the ratios and orientations of the principal stresses that cause the earthquakes. Although we have not carried out such an analysis, it is clear from the similarity of the fault plane solutions that faults of different orientations are being activated by a uniform stress field.

SEISMIC SOURCE PARAMETERS

To quantify the physical sizes of the faults and the amounts of slip that accompany the microearthquakes, seismic source parameters were determined from the spectra of waveforms recorded by the triaxial sensor located in EE-1 (see Figure 1). Spectra were calculated by choosing a portion of the waveforms and computing the Fourier transform. The spectra were interpreted using the models of Brune (1970) and Aki (1966). Source parameters, such as source radius, seismic moment, stress drop, and amount of slip across the fault during the microearthquake can be determined from these models using measurements of the low frequency spectral amplitude and corner frequency of the displacement spectra.

Figure 5 shows a waveform of a typical microseismic event recorded by the sensor in EE-1. The three components of particle motion have been rotated to produce the component of motion that is parallel to the line joining the source and receiver. Also shown in Figure 5 is the spectrum of ground displacement for the first .08 s portion of the P wave. The low frequency spectral amplitude and corner frequency are labeled in the figure.

Computed seismic moments for the events studied range from 10^{21} to 10^{23} dyne cm. Source radii range between 2 and 20 m, stress drops range between .5 and 50 bars, and average displacements across the faults vary from 6 to 1000 microns. These microearthquakes are very small indeed! For comparison, the 1964 Alaska earthquake, with a magnitude of 9.2 (Mw), is estimated to have had a seismic moment of 8.2×10^{29} dyne-cm, a fault dimension of 500 km and an average slip of 700 cm (Kanamori, 1971, 1977). Given the small amount of displacement accompanying the microearthquakes, it is unlikely that a significant increase in permeability accompanies their occurrence.

SEISMIC VELOCITY AND ROCK ANISOTROPY

To determine seismic velocities for locating the microearthquakes, and to establish travel time corrections to stations, detonators were placed in the borehole EE-2 in the region near where the fluid was injected into the rock.
By moving the position of the detonator in the borehole it is possible to determine if significant variations in travel times to stations occur that can be interpreted in terms of the rock heterogeneity.

A large scale, cross wellbore experiment was conducted during earlier hydraulic fracturing studies in two wellbores, EE-1 and GT-2, located near EE-2. In this experiment a moving seismic source was placed in one wellbore and a stationary receiver in the other, the source was fired every 2 cm along the wellbore. In this way, a large volume of rock between the boreholes could be studied in detail. The results showed that little heterogeneity existed in the rock prior to hydraulic fracturing but that significant inhomogeneities existed after fracturing and sub

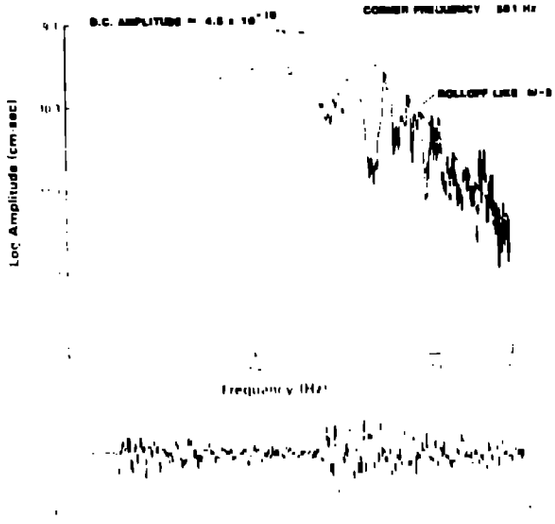

Figure 5. Waveform (below) and spectrum (above) of first .08 s of P wave for a typical microseismic event. Spectrum was smoothed (line) to determine parameters that were input to the Brune (1970) model.

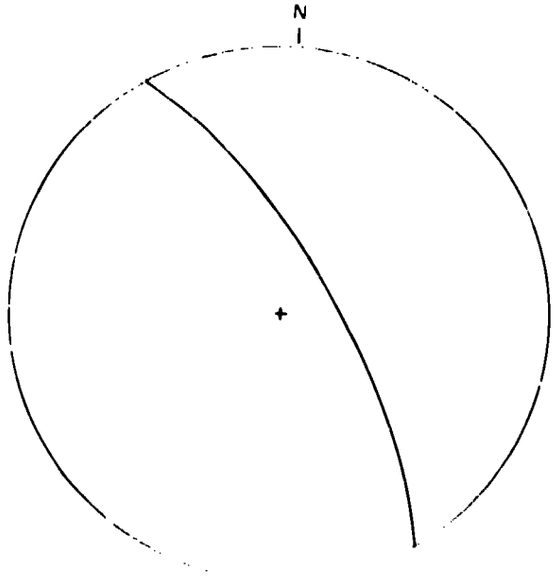

Figure 6. Lower hemisphere stereo projection of plane that is parallel to the most sets of locations of microseismic events.

sequently extracting heat from the region between the two wellbores (Fehler, 1981; Aki, et al 1982; Pearson, et al, 1983). Spatial variations in velocity of as much as 10% were found in the previously homogeneous rock.

In the region where microearthquakes were found during Experiment 2032, temperatures are too high to allow a detailed cross well experiment to be carried out. An alternative approach is to use the microearthquakes themselves as sources to study the three dimensional heterogeneity of the region in and near where the microearthquakes occurred. In principle, it should be possible to construct a complete three dimensional tomographic image of the region using the microearthquakes as sources.

As a first, crude, attempt at constructing an image of the seismic zone, the microearthquakes were grouped by region of occurrence and a joint location scheme (Crosson, 1976) was used to determine improved relative locations and station corrections to the five station network used to locate them. The station corrections in this scheme are those specifically calculated for the events in the subregion under study. Relative differences in station corrections among the regions studied can be interpreted in terms of velocity heterogeneities along paths from the various regions to the seismic stations. Preliminary results indicate that there are path anomalies to stations that are consistently detected. Interpretation is difficult at this time because of the fact that station corrections are always calculated with respect to corrections for other stations.

Roberts and Crampin (1986) have studied the three dimensional particle motion of S waves recorded from microearthquakes accompanying a hydraulic fracturing experiment by the British Hot Dry Rock Project. They find convincing evidence of anisotropy in the rock (granite) between the source and receiver. This anisotropy is manifested by a birefringence of the S wave that can be identified from the particle motion of the initial portion of the S wave. Roberts and Crampin (1986) argue that this anisotropy is caused by a preferential orientation of fractures in the rock. The orientation of the fractures deduced from the S wave data agrees with the orientations of fractures measured near the surface and interpretations of televiewer logs in boreholes.

DETERMINING JOINT ORIENTATIONS

Because microearthquakes were located with a precision of 10-20 m, it is possible to study the relative locations of the events to determine if several microearthquakes occurred along a single pre existing joint in the rock. In addition, if a system of parallel joints exists along which microearthquakes occur, it should be possible to determine the orientation of this joint system by studying the relative locations of the microearthquakes.

Lutz (1986) proposed that an underlying structure controlling the locations of mapped points on the surface of the earth could be revealed by calculating the azimuths of all possible pairs of points that comprise the field data set and compiling a histogram of the number of point pairs giving a specified azimuth. Since the resulting histogram is strongly biased by the shape of the region in which the points occur, what Lutz calls a shape effect, studies of synthetic data that are randomly located within a region that has the same shape as the study area must be carried out. Lutz proposes that an equal number of points be randomly placed within the region and a histogram of the azimuths of lines connecting pairs of points in the random data set be computed. By studying a large number of sets of the randomly distributed data located in a region with the same shape as the field region, a distribution of histograms can be compiled, one histogram for each set of random data. In this way, some estimate of the effects of the study region shape on the calculated field data histograms can be made. Lutz proposes that the histogram for the field data be compared with a mean histogram, which is an average of all the histograms obtained from the different sets of random data. The level of confidence in the result can be estimated by comparing the histogram compiled from the field data with the distribution of histograms from the random data.

In the present study, data are located in three dimensions. We seek to determine the dips and azimuths of planes along which multiple microearthquakes occur. Since three points are required to define a plane, we searched for all possible sets of three points in the location data set and calculated the dip and azimuth of the plane connecting the three points. For N data points, there are

$$N\cdot(N-1)\cdot(N-2)/6$$

possible sets of three points. For 844 microquakes, there exist 10⁸ possible sets, so to reduce this large number somewhat and to search for a more realistic model of joints, we considered only sets of points that were all located within 200 m of each other. (We also considered cases of 100 m and 50 m which yielded results similar to those presented).

To remove the shape effect as described above, we produce sets of random points located within the seismic region. The azimuths and dips of sets of these randomly located events were calculated and compared with the results of the actual data. We used 100 sets of randomly located events, each set containing exactly the same number of locations as in the real data set, e.g. 844 locations.

Our comparison of the histogram of number of event planes with a given dip and azimuth with the mean histogram compiled from all 100 sets of randomly located events showed one dominant peak in the data, whose amplitude is 2.2 times the amplitude of the peak in the same direction in the average of the random data sets. In fact, the peak has a much higher amplitude than the peak for any of the random data sets studied. This gives us a strong confidence that the dip and azimuth determined from the real data are reliable.

Tests using synthetic data where points are chosen to line up along randomly located but parallel joints show that the technique described above does yield a reliable estimate of the dip and azimuth of the planes along which the points lay.

The predominant azimuth of the planes joining the most microearthquakes is 35° west of north. The planes dip 75° to the east. One such plane is shown in a lower hemisphere stereo projection in Figure 6. This plane is nearly parallel to the plane that is common to the fault plane solutions shown in Figure 4. In fact, this plane would fit exactly the data shown for the Group I fault plane solution shown in Figure 4. Thus, the fault orientations determined by the fault plane solutions agree well with the joint orientations determined from locations. This adds confirmation to our assertion that the microearthquakes occur along pre-existing joints.

Visual confirmation of the preferential orientations of the microearthquakes can be seen in Figures 7 and 8, which show a portion of the microearthquake location data sets. Figure 7 is an epicenter map showing locations of events that occurred during the first 20 hours of the injection. There is a clear trend in the location pattern in a direction N35°W that occurs NW of the wellbore. Figure 8 shows a vertical cross section of the microearthquake locations projected on a plane trending N55°W, along the strike of the preferential direction of joints as determined above. In this figure, planes that define the joint pattern should dip 75° to the right and many such planes can be seen in the figure.

CONCLUSIONS

Seismic data collected during hydraulic fracturing provide estimates of earth stresses and rock physical properties which are independent of, and thus supplement conventional analysis of pressure records and impression packer or televiewer data. Seismic measurements are not limited to the immediate vicinity of the wellbore and, in fact, large volumes of rock can be interrogated by the seismic technique.

Fault plane solutions gave a good indication of the direction of least compressive stress. In addition, the fault plane solutions can be studied to obtain additional information about the stress field. The earthquake location patterns indicated a preferred direction of fault planes which is consistent with one of the fault planes determined in the fault plane solutions. Finally, the slips estimated to accompany the seismic events are very small; hence the microseismic events contribute very little increased permeability in the rock volume.

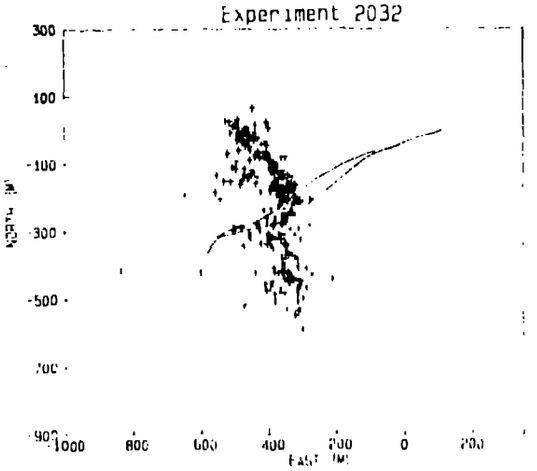

Figure 7. Map view of locations of microseismic events accompanying the first 20 hours of water injection. Note the N35oW trend of the locations in the upper portion of the figure.

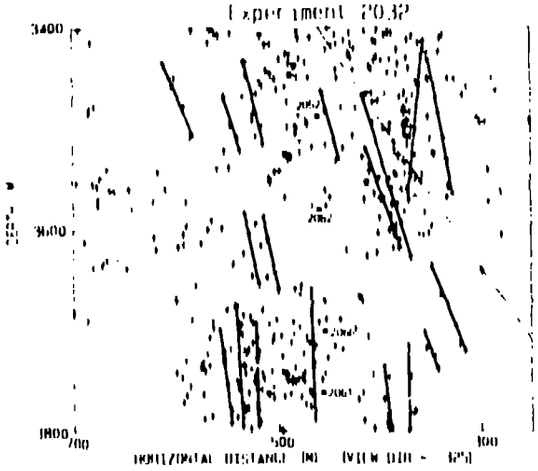

Figure 8. Vertical cross section showing locations of microseismic events projected onto a vertical plane trending N55°W. Note the many groups of events that can be connected by nearly vertical lines which are parallel to the preferred direction of orientation found by statistical analysis.

ACKNOWLEDGMENTS

We gratefully acknowledge the cooperation of the entire staff of the Los Alamos Hot Dry Rock Program. In particular, we thank Hugh Murphy for useful discussions and encouragement and Evon Stephani for supervising instrumentation. This work was funded by the U.S. Department of Energy and the governments of Japan and the Federal Republic of Germany.

REFERENCES

Albright, J.N., and Hanold, R.J., 1976, "Seismic Mapping of Hydraulic Fractures in Basement Rocks," Proc. 2nd RFDA Enhanced Oil and Gas Recovery Symposium.

Albright, J.N. and Pearson, C., 1982, "Acoustic Emissions as a Tool for Hydraulic Fracture Location: Experience at the Fenton Hill Hot Dry Rock Site," Soc. Petr. Eng. J. pp. 523-530.

Aki, K., 1966, "Generation and Propagation of G Waves from the Niigata Earthquake of June 16, 1964," Part 1, Bull. Earthquake Res. Institute, Vol. 44, pp. 23-72.

Aki, K., et al., 1982, "Interpretation of Seismic Data From Hydraulic Fracturing Experiment at the Fenton Hill, New Mexico, Hot Dry Rock Geothermal Site," JGR, Vol 87, No. B2, pp. 936-944.

Aldrich M., and Laughlin, A.W., 1984, "A Model for the Tectonic Development of the Southeastern Colorado Plateau Boundary," J. Geophys. Res. 89, pp. 10207-10218.

Batchelor, A.S., Baria, R., and Hearn, K., 1981, "Monitoring the Effects of Hydraulic Stimulation by Microseismic Event Location: A Case Study," Society of Petroleum Engineers, 12109.

Brune, J., 1970, "Tectonic Stress and the Spectra of Seismic Shear Waves from Earthquakes," J. Geophys. Res. 75, pp. 4997-5009.

Cash, D., et al., 1983, "Fault Plane Solutions for Microearthquakes Induced at the Fenton Hill Hot Dry Rock Geothermal Site: Implications for the State of Stress Near a Quarternary Volcanic Center," Geophys. Res Letters, IV, pp. 1141-1144.

Cornet, F.H., and Valette, B., 1984, "In Situ Stress Determination from Hyraulic Injection Test Data," J. Geophy. Res., 86, pp. 11527-11538.

Crosson, R.S., 1976, "Crustal Structure Modeling of Earthquake Data 1. Simultaneous Least Squares Estimation of Hypocenters and Velocity Parameters", J. Geophys. Res. 81, pp 3036-3046.

Fehler, M., 1981, "Changes in P Wave Velocity During Operation of a Hot Dry Rock Geothermal System", J. Geophys. Res. 86, pp. 2925-2928.

Gephart, J.W., and Forsyth, D.W., 1984, "An Improved Method for Determining the Regional

Stress Tensor Using Earthquake Focal Mechanism Data: Application of the San Fernando Earthquake Sequence," J. Geophys. Res. 89, No. B11, pp. 9305-9320.

Haimson, B., and Rummel F., 1982, "Hydrofracture Stress Measurements on the Iceland Research Drilling Project Drill Hole at Reydarfjordur, Iceland," J. Geophys. Res. 87, pp. 6631-6649.

House, L., Keppler, H., and Kaieda, H., 1985, "Seismic Studies of a Massive Hydraulic Fracturing Experiment," Trans. Geotherm. Res. Council.

Kanamori, H., 1977, "The Energy Release in Great Earthquakes," J. Geophys. Res. 82, No. 20.

Kanamori, H., 1971, "Great Earthquake at Island Arcs and the Lithosphere," Tectonophysics 12, pp. 187-198.

Lutz, T.M., 1986, "An Analysis of the Orientation of Large-Scale Crustal Structures: A Statistical Approach Based on Areal Distributions of Pointlike Features," J. Geophys. Res., 91, No. B1, pp. 421-434.

Michael, A.W., 1984, "Determination of Stress from Slip Data: Faults and Folds," J. Geophys. Res., 89, pp. 11517-11526.

Pearson, C., 1981, "The Relationship Between Microseismicity and High Pore Pressure During Hydraulic Stimulation Experiments in Low Permeability Granitic Rock," J. Geophys. Res. 86, pp. 7855-7864.

Pearson, C., 1982, "Source Parameters and a Magnitude Moment Relationship from Small Local Earthquakes Observed During Hydraulic Fracturing Experiments in Crystalline Rocks", Geophys. Res. Let., 9, pp. 404-407.

Pearson, C., Fehler, M., and Albright, J., 1983, "Changes in Compressional and Shear Wave Velocities and Dynamic Moduli During Operation of a Hot Dry Rock Geothermal System", J. Geophys. Res., 88, pp. 3468-3475.

Pine, R.J., and Batchelor, A.S., 1984, "Downward Migration of Shearing in Jointed Rock During Hydraulic Injections," Int. J. Rock Mech. Min. Sci. & Geomech. Abstr. Vol 21, No. 5, pp. 249-263.

Roberts, G. and Crampin, S., 1986, "Shear-Wave Polarizations in a Hot-Dry Rock Reservoir: Anisotropic Effects of Aligned Cracks", Int. J. Rock Mech. Min. Sci. & Geomech. Abtr., in press.

Stock, J.M., et al., 1985, "Hydraulic Fracturing Stress Measurements at Yucca Mountain, Nevada, and Relationship to the Regional Stress Field", J. Geophys. Res., 90, pp. 8691-8706.